



Development of a Young's modulus model for Gilsocarbon graphites irradiated in inert environments

Ernest D. Eason^{a,*}, Graham N. Hall^b, Barry J. Marsden^b, Graham B. Heys^c

^a Modeling and Computing Services, P.O. Box 18583, Boulder, CO 80308, USA

^b Nuclear Graphite Research Group, School of Mechanical, Aerospace and Civil Engineering, University of Manchester, P.O. Box 88, Manchester M60 1QD, UK

^c HM Nuclear Installations Inspectorate, Health and Safety Executive, Building 3, Redgrave Court, Merton Road, Bootle, Merseyside L20 7HS, UK

A B S T R A C T

Dimensional and material property changes caused by fast neutron damage, radiolytic oxidation or a combination of both have been measured over many years on the Gilsocarbon graphites. The data have been gathered together in a comprehensive database and are being used to develop dose–damage relationships of irradiated graphite material properties for use in irradiated graphite component stress analyses up to a fast neutron dose of $\sim 200 \times 10^{20}$ n/cm² equivalent DIDO nickel dose (EDND) in the temperature range ~ 300 – 650 °C. This paper covers development and validation of an empirical model for Young's modulus of Gilsocarbon graphite when irradiated in an inert environment. The new model provides a good fit over the range of the primary modelling variables: dose, irradiation temperature, and graphite group. The proposed model is convenient to use in component stress analysis, as it features an analytic function of temperature and dose that eliminates the need in the existing model for interpolation on those variables.

© 2008 Elsevier B.V. All rights reserved.

1. Introduction

Graphite components manufactured from Gilsonite coke, which is usually referred to as Gilsocarbon, have been used as moderators in the Advanced Gas Cooled Reactors (AGR) in the UK, the THTR in Germany and as fuel supports in some French Magnox reactors. The effect of fast neutron irradiation in a reactor leads to changes in the structural, mechanical and thermal properties of Gilsocarbon [1]. In a carbon dioxide cooled reactor these properties are further affected by ionising radiation (gamma and neutron) in combination with the coolant gas, leading to radiolytic oxidation [2]. Property changes also depend on irradiation temperature, coolant composition, and direction of loading relative to the grain structure.

The methodology currently employed in modelling graphite behaviour for nuclear graphite component stress analysis is an empirically based approach, which relies on a variety of assumptions and scaling factors to relate data from Materials Test Reactors (MTRs) to the operational behaviour. The Gilsocarbon graphite behaviour models in use at present are based on fits to a limited set of MTR data such as those present in Ref. [1]; in this paper these earlier models are referred to as 'Existing Fits'.

The work reported here is part of a broader data collection and analysis effort, in which statistical and pattern recognition tools are used to develop dose–damage relationships for the key material properties and dimensional changes. The overall effort includes collecting and reviewing all of the available irradiation data obtained over many years at the UKAEA [3] on Gilsocarbon materials. This has produced a comprehensive database, including all relevant variables (numeric) and factors (non-numeric) such as dose, irradiation temperature, density, graphite material identifying code or type, grain direction, irradiation atmosphere, etc. The available data are being analysed to determine which variables and factors are statistically significant and to identify the trends in the data in order to produce improved irradiation models. Such an approach also aids understanding and points to areas where further data or research is required.

This paper summarises the modelling and analysis work on the Young's modulus of Gilsocarbon graphite when irradiated in an inert environment. The database development and dimensional change modelling already completed have been previously reported in [4] and are only briefly mentioned here.

2. Dataset development

The collection and review of data and the development of the individual property datasets were conducted at the University of Manchester by the Nuclear Graphite Research Group. The process

* Corresponding author. Tel.: +1 303 530 4295; fax: +1 303 530 3945.

E-mail addresses: eeason@ix.netcom.com (E.D. Eason), graham.n.hall@manchester.ac.uk (G.N. Hall), barry.marsden@manchester.ac.uk (B.J. Marsden), Graham.Heys@hse.gsi.gov.uk (G.B. Heys).

undertaken is not discussed in this paper, but the end result is approximately 22,000 data points that encompass 17 material properties of 88 types of graphite (i.e., different identifying codes), all based on Gilsocarbon coke, in six environment/loading conditions (virgin, irradiated, pre-radiolytically oxidised, radiolytically oxidised, combined irradiation and radiolytic oxidation, and tripanned from AGR operating plants) over a temperature range of 350–600 °C. Additional data are available outside these temperatures, spanning the range 150 °C to about 1400 °C. Extension of the models described here to fit higher temperature data could be of interest for very high temperature reactor (VHTR) development.

The Young's modulus dataset in the 300–650 °C range includes about 950 data points with measured modulus ratio E/E_0 in an inert environment, with an Equivalent DIDO Nickel Dose (EDND) of up to 367×10^{20} n/cm². Of these, about 600 observations are for moderator materials relevant to present operating reactors, and most of these observations are sufficiently complete to be usable for model calibration, validation, or comparison purposes. The dataset for combined irradiation and radiolytic oxidation environments is much smaller, so modelling the inert environment data is a reasonable first step toward a complete model of the effects of irradiation on the modulus of Gilsocarbon graphite irradiated in an oxidising atmosphere.

2.1. Modelling variables

Several variables were considered in the modelling process, but the final choices are modulus ratio E/E_0 as the dependant variable and dose, irradiation temperature, and graphite group as the independent modelling variables. The modulus ratio was chosen instead of irradiated modulus because more data are available with that choice. Values of irradiated modulus, E , and unirradiated modulus, E_0 , are not always documented, yet the ratio almost always is. The possibility of bias in estimating irradiated modulus from a model of the modulus ratio was analysed in the exploratory modelling stage, as reported below, and no bias was found. Analysis conducted after model calibration confirmed that dose, T_{irr} , and graphite group are the key independent variables, and additional variables including measurement direction relative to the grain, flux, and unirradiated density are not needed in the modulus model. The three chosen modelling variables are reasonably numerically independent of each other in the available data, which is important for numerical stability in fitting the data.

It should be noted that measurement direction relative to the grain structure is an important variable for the dimensional change model in [4], but not for Young's modulus in moulded Gilsocarbon. Extruded Gilsocarbon materials show more anisotropy than moulded Gilsocarbon and do need to consider grain direction. Although a significant amount of extruded Gilsocarbon graphite was irradiated in various MTR programmes, it was not chosen as a moderator material for power producing reactors. Hence the extruded graphite groups identified in the exploratory modelling phase are not considered further in this paper.

2.2. Grouping of graphites for analysis

Many different Gilsocarbon graphite codes were used historically to identify specific materials, some of which correspond to the same or very similar material. Data with various graphite codes were combined into nine graphite groups for analysis, such that each group contains graphites used in the core at specific nuclear plants (or not so used, in the case of extruded groups). Within each group, all materials were made by the same forming techniques

(moulded, extruded, and pressed), and with similar initial density. Additional graphite groups contain data with unknown measurement direction and other missing information, and in some cases, special graphite grades made for research purposes, which were not used in any nuclear plant. All of the data on materials (groups) that were not used as moderator graphites in existing power stations were set aside and not used in calibration and validation procedures. Thus, the Young's modulus curves that are identified with a particular power station are not biased by data on materials which may be used in a different station or for research purposes.

2.3. Separation of data into calibration and validation sets

After defining the graphite groups, the modulus dataset was randomly split prior to the modelling process into a 90% calibration subset and a 10% validation subset. The purpose was to reserve a sample of data that were not used in model development to provide proof that the fitted model has predictive capability. Unfortunately, too many of the points nearest the maximum amplitude of the Young's modulus vs. dose curves happened to be randomly selected for the validation subset. This could have caused underestimation of the amplitude in the calibration process. Consequently, following the exploratory modelling phase, where this situation was detected, nine points were moved from the validation set to the calibration set. The result is that the final validation set is not a purely random sample. However, the remaining validation points are still a sample of the initially available data, and they were set aside and not used in modelling, so they still provide useful evidence that the model can predict data not used in fitting.

3. Young's modulus model

The analysis steps included exploratory modelling, preliminary model review, final model calibration, and validation. Candidate modelling variables, grouping of graphites, use of the dose ratio, and other modelling aspects from the dimensional change modelling effort were considered for possible relevance to the modulus model in the exploratory modelling phase. Following the exploratory modelling, a review of the preliminary modulus model was conducted by the authors and representatives from the nuclear industry. A number of questions were raised concerning the preliminary model, which were answered by additional analysis before proceeding to final model calibration and validation. Selected findings from the exploratory modelling and model review steps are briefly summarized below.

3.1. Model of turnaround dose

The dose at the minimum (turnaround) of the dimensional change vs. dose curves proves to be a useful parameter in both dimensional change and Young's modulus modelling. The parameter was originally analysed as part of the dimensional change modelling effort. The dependence on temperature was characterised using a pattern recognition tool, and a simple model was developed for the dose at minimum dimensional change, $EDND_m$, which is also referred to as turnaround dose, as presented in [4]. The turnaround dose depends on measurement direction relative to the grain as well as temperature of irradiation, as shown in Eq. (1)

$$EDND_m = f(\text{direction})(2211 - T_{irr})^{3.17} \quad (1)$$

This form gives a reasonable fit within the range of temperatures of interest to UK power stations, approximately 300–600 °C, and also up to about 1100 °C. The shape of the function is shown in Fig. 1.

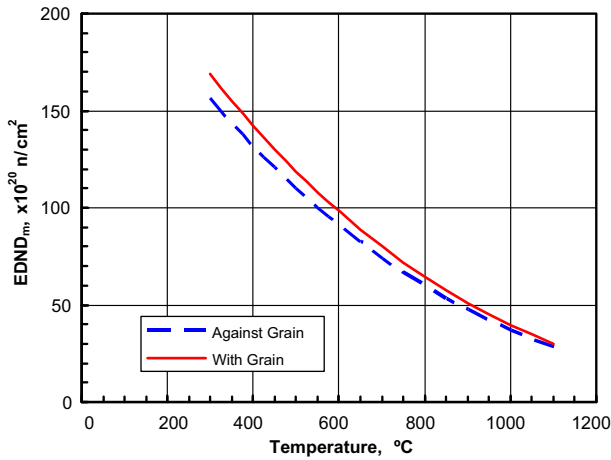


Fig. 1. Model of turnaround dose, EDND_m.

3.2. Definition of dose ratio, DR

A dimensionless dose ratio (DR) is defined as the actual dose (EDND, n/cm² units) divided by the turnaround dose EDND_m given by Eq. (1), i.e.,

$$DR = EDND/f(\text{direction})(2211 - T_{\text{irr}})^{3.17}. \quad (2)$$

The reason for defining the dose ratio is the observation during exploratory dimensional change modelling that the different shapes of dimensional change vs. dose curves at various temperatures nearly coincide in a ‘master curve’ if expressed in dose ratio units. Because data at many temperatures can be modelled together, the subsequent modelling steps are simplified. Exploratory modelling of the Young’s modulus data revealed that the same benefit is obtained by using dose ratio to model the increase in Young’s modulus with irradiation in inert environments. The greatest increase in the Young’s modulus occurs at a consistently higher dose than the dimensional change turnaround at each irradiation temperature, and the dependence of that maximum-modulus dose on T_{irr} is similar to the dependence of dimensional change turnaround dose on T_{irr} . Thus, the dose ratio expression developed for dimensional change (Eq. (2)) is useful for modulus modelling as well. The Young’s modulus is not as sensitive to anisotropy as is

dimensional change, so the value used for $f(\text{direction})$ in the modulus model is the average of the values for against-grain and with-grain directions as determined for the dimensional change model.

3.3. Results of preliminary model review

In this section, selected results of the model review are presented. The model used for investigating these issues was a preliminary model, but the conclusions should hold for the final model as well.

One of the questions in the preliminary model review was whether modelling the modulus ratio E/E_0 could introduce bias, compared to modelling the irradiated modulus E directly. To answer this question, the subset of observations in the database that included recorded values of both E and E_0 was analysed by comparing the actual measured E and the value of E estimated by multiplying the E/E_0 model by the measured value of E_0 for each point. Using the point-by-point recorded value of E_0 , the result should be the same (within modelling error) as using the actual measured E , and it is, as shown in Fig. 2(a).

In actual applications, the estimate of E/E_0 from the model would be multiplied by a tabulated value of E_0 for the particular power station graphite to provide an estimate of E , because there would be no measured value of E_0 corresponding to each model prediction. Average values of E_0 for each station graphite are available, based on the heat certificate records supplied by the graphite manufacturer during production, and these data are reasonably independent of the model of E/E_0 and the recorded values of E . Multiplying these station values of E_0 by the model estimate of E/E_0 provides a second estimate of irradiated E , which can be compared to the recorded E measurement as shown in Fig. 2(b). As should be expected, using values tabulated by power station introduces somewhat greater scatter than using the individually measured values for each point, but there is no apparent systematic bias relative to the 1:1 line. Since no substantial bias is evident by either the point-by-point or station-tabulated E_0 methods in Fig. 2, the conclusion is that the model of E/E_0 does not introduce bias compared to modelling E directly.

Another question concerned the use in this work of an additive model, where the initial increase in modulus to a value P at very low dose is added to the subsequent increase in modulus with additional dose, Δ , to get the value of E/E_0 at any point, as shown in Fig. 3.

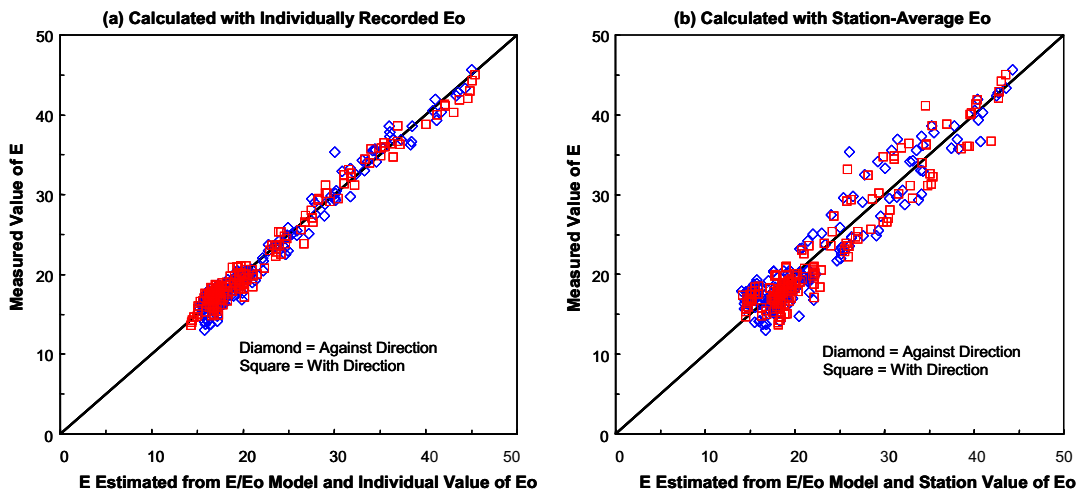


Fig. 2. Comparison of measured irradiated E with estimated E from E/E_0 model and (a) measured point-by-point E_0 , and (b) independently tabulated E_0 for each power station graphite.

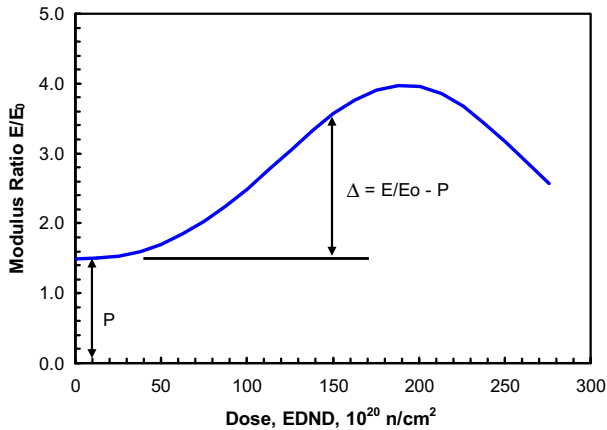


Fig. 3. Schematic of additive model $E/E_0 = P + \Delta$.

In the existing modulus model, the initial 'pinned' value P and a tabulated function describing the subsequent increase with dose (the structure term S) are multiplied together. Analysis shows that the two approaches are algebraically equivalent if the tabulated structure term is defined as $S = 1 + \Delta/P$, where Δ is the increase above P in the additive model. Thus, with this definition of the structure term, there is no inconsistency between the new additive model form and the existing multiplicative model form.

Additional issues were raised concerning the model form, including possible dependence of various parts of the model on measurement direction, T_{irr} , and flux. The results of these investigations are embodied in the final model form and discussion of variable dependencies, given below. A companion paper discusses the flux effects and validity of using a flux-adjusted temperature, Equivalent DIDO temperature (EDT) for modelling [5]. The existing model is based on EDT, while the new model is based on actual irradiation temperature, T_{irr} .

3.4. General Young's modulus model form

A convenient fitting form with sufficient flexibility to fit Young's modulus data as a function of many different temperatures and graphite types, in both measurement directions, is given by the following equation

$$\frac{E}{E_0} = P + A \left(\frac{DR}{B} \right)^{C-1} \exp \left[- \left(\frac{DR}{B} \right)^C \right]. \quad (3)$$

In addition to DR , defined in Eq. (2), there are four fitting functions in this model form, P , A , B , and C . All four are functions of irradiation temperature, T_{irr} , and P , A , and B also depend on graphite group. P is called the 'pinning' term, and it is defined for this model as the value of E/E_0 at a dose of about 10^{21} n/cm² (this is at or near the lowest recorded dose in many test data series, so it is a practically-defined 'low dose'). A is the amplitude function, B controls the dose at which maximum amplitude is reached, and C varies the shape of the function with T_{irr} .

A graphical interpretation of the four fitting functions is given in Fig. 4. The same model curves shown on Fig. 4 as a function of dose are also shown as a function of dose on Fig. 5. It is clear that lower irradiation temperature causes the peak modulus ratio to decrease in amplitude and shift to a higher dose, an effect that is reasonably well captured by the dose ratio approach.

4. Comparison of Young's modulus model and data

For each of the reactor moderator graphite groups, the calibrated Young's modulus model has been compared with the data

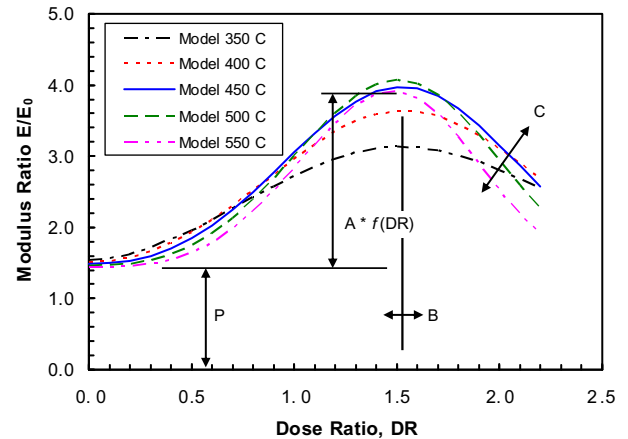


Fig. 4. Schematic of Young's modulus model fitting functions.

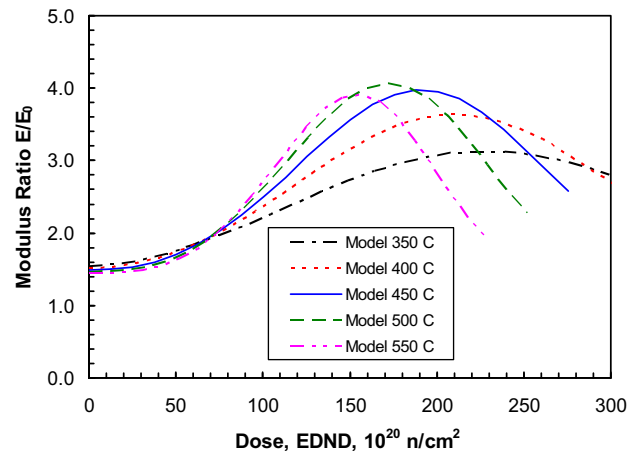


Fig. 5. Same model curves as in Fig. 4 expressed in terms of dose instead of dose ratio.

at various irradiation temperatures, examples of which are given below. Fig. 6(a)–(d) show that the model corresponds well to data for graphite group 2 over the temperature range 390–600 °C. There is no obvious direction effect for this graphite group, as shown by the datapoints in Fig. 6, which are often nearly coincident in the against-grain (A) and with-grain (W) directions. Where the data in the two directions are not coincident, there is no consistent pattern of A being higher than W or vice versa, which is typical of modulus results with the moderator graphites. Additional comparisons with another moderator graphite group are given below in Fig. 8, which show the same lack of a direction effect.

Based on Fig. 6 (and additional comparisons for each graphite group and temperature range with sufficient data), the model is clearly able to change the curve shape as a function of irradiation temperature and graphite group to match the data. In most cases, the agreement between the data and the relevant curve is quite good. It should be noted that the irradiation temperature and dose dependence of the new model is an overall function based on data from all temperatures and all moderator graphite groups, rather than being separately optimised for specific temperatures or individual groups. The fitting constants that vary by group provide the means to approximately adjust the overall function for the effects of group differences.

The dashed curves on Fig. 6 are the existing model, discussed in greater detail below. The existing model fits some of the data from graphite group 2 about as well as the new model, but other dose-

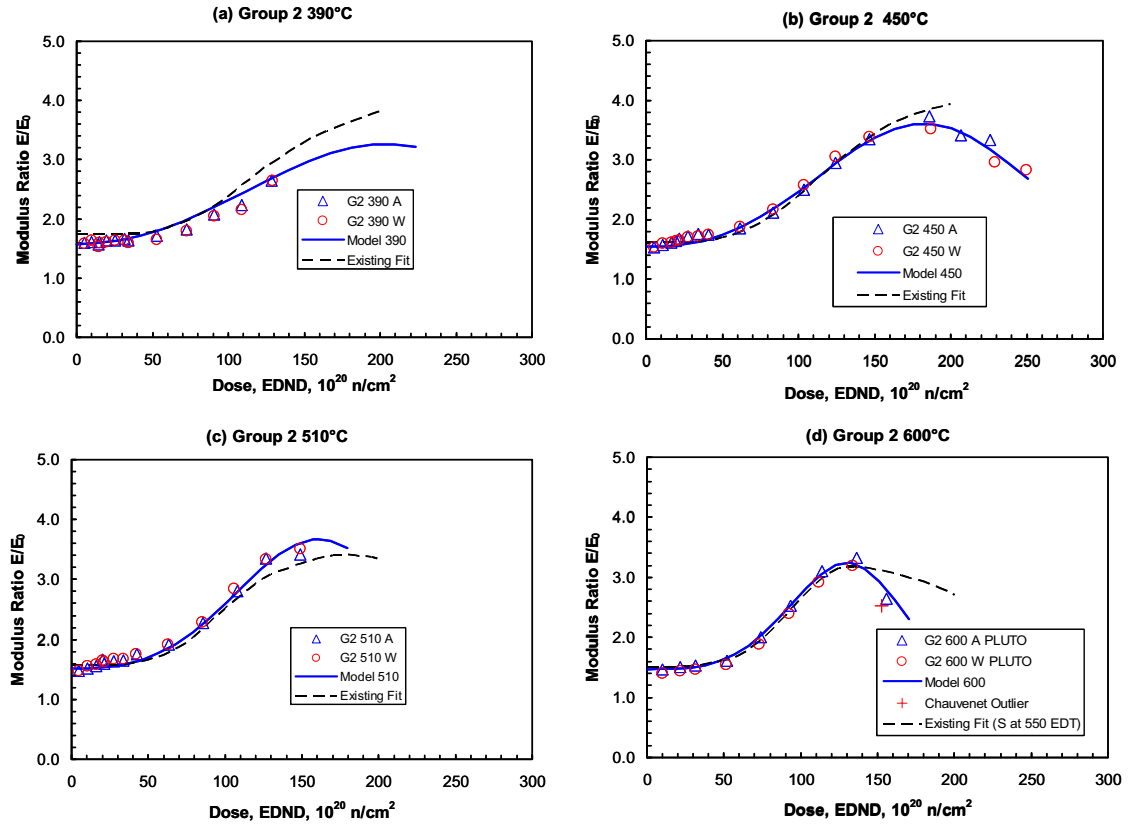


Fig. 6. Young’s modulus model compared with data on graphite group 2 at various irradiation temperatures (a) 390 °C, (b) 450 °C, (c) 510 °C, and (d) 600 °C. The dashed curve is the existing modulus model prediction.

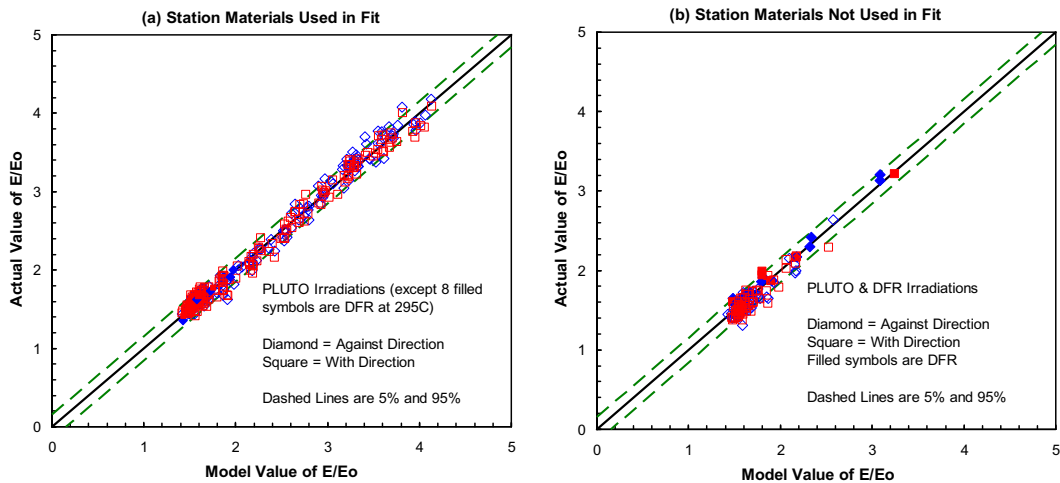


Fig. 7. Actual versus model values of E/E_0 for (a) data used for calibration and (b) data not used for calibration.

temperature ranges are fitted better by the new model, shown by the solid curve.

4.1. Quality of fit

There are several ways to assess the quality of the least squares fit for the new model. A standard approach is to compare the model graphically with the data in appropriate temperature and graphite groups, as shown by Fig. 6. In many such comparisons over the range of dose, irradiation temperature and graphite groups, there is generally good agreement between the data (in both against-grain and with-grain directions) and the new model.

A more quantitative comparison can be made using the standard error of the model. Over the entire calibration set (390 points), the standard error is $S_e = 0.09$ (measured as E/E_0). Typical modulus ratio values are in the range $E/E_0 = 1.5$ – 4 , so the model estimates the typical modulus ratio with a $1S_e$ uncertainty of about 2–6%.

Another approach for evaluating goodness of fit, which takes all model variables into account on a single plot, is to compare model estimates of E/E_0 and actual measured E/E_0 . A perfect fit with no scatter would have all data on the solid 1:1 line shown in Fig. 7. In reality, there is always some scatter about the 1:1 line, so dashed lines are plotted in Fig. 7 representing 5th and 95th percentiles of a

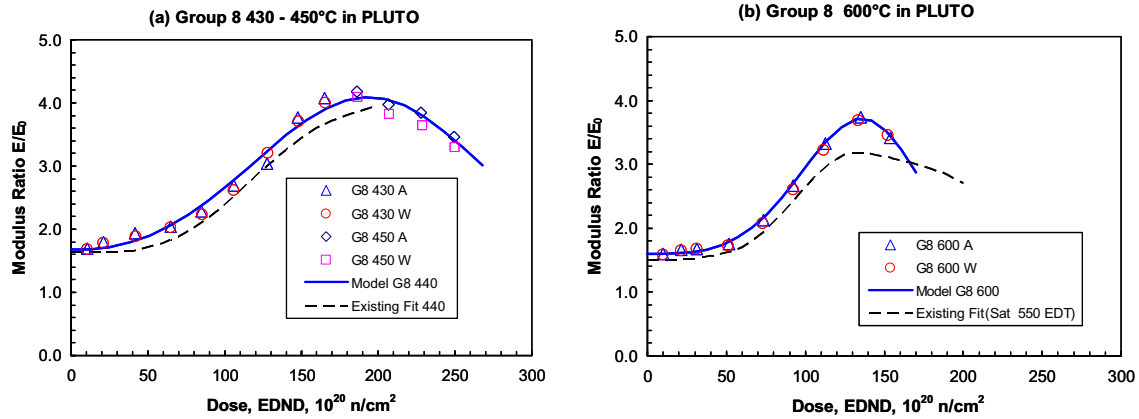


Fig. 8. Comparison of models and data on graphite group 8, (a) at $T_{\text{irr}} = 440^\circ\text{C}$ and (b) at $T_{\text{irr}} = 600^\circ\text{C}$. The solid curve is the new model and the dashed curve is the existing fit.

normal distribution about the 1:1 line with a standard deviation $SD = 0.09$. A normal distribution assumption is reasonable, based on analysing the residuals. From the fact that the calibration points in Fig. 7(a) scatter close to the 1:1 line, mainly within the dashed bounds and without obvious under or over prediction, it is apparent that the model provides a good estimate of actual E/E_0 over the range of the data.

Residual plots were also generated, plotting the residuals (difference between each data point and the model) against each variable as another indication of quality of fit. The residual plots for variables that are in the model did not give any indication of inaccurately modelled trends, and residual plots for independent variables not in the model did not identify any un-modelled trends that would suggest that additional variables should be added to the model.

4.2. Model validation

The validation points that were not used in model development show excellent agreement with the model as shown in Fig. 7(b). The standard deviation of residuals about the model for data not used in calibration is $SD = 0.093$, essentially the same as $SD = 0.091$ for the calibration set, indicating an equally good fit. This result proves that the model is capable of predicting data that were not used in model development about as well as it fits the calibration data used to develop the model.

4.3. Comparison with the existing model of Young's modulus

The existing model of Gilsocarbon Young's modulus is designed to interpolate on temperature in two tables of values, one for the initial increase in modulus at low dose (the pinning term, P) and another for the subsequent increase in modulus at higher dose (the structure term, S). In the structure term table it is also necessary to interpolate on dose. The curves for the existing structure term model are given in tabular form at several equivalent DIDO temperatures (EDTs) in the range $350 \leq \text{EDT} \leq 550^\circ\text{C}$ and for various doses up to $200 \times 10^{20} \text{ n/cm}^2$ EDND. The relationship between actual irradiation temperature, T_{irr} , and EDT depends upon the test reactor flux, ϕ , so that different test reactors have different EDT at the same actual irradiation temperature according to Eq. (4). The activation energy used in Eq. (4) is $E = 1.2 \text{ eV}$ for the pinning term and $E = 3.0 \text{ eV}$ for the structure term, EDT and T_{irr} are absolute temperatures (K), and flux ϕ is in units of $\text{n/cm}^2/\text{s}$

$$\frac{1}{\text{EDT}} - \frac{1}{T_{\text{irr}}} = \frac{8.617 \times 10^{-5}}{E} \ln\left(\frac{\phi}{4 \times 10^{13}}\right). \quad (4)$$

For comparison with data from inert environments and the new model, the existing fit with no weight loss is used, i.e., $E/E_0 = P \times S$.

Fig. 8(a) and (b) shows comparisons of the existing model and the new model for graphite group 8. All of the data in Fig. 8 are from irradiation in the PLUTO test reactor, for which $T_{\text{irr}} = 440^\circ\text{C}$ corresponds to 397°C EDT for the pinning term and 422°C EDT for the structure term. At $T_{\text{irr}} = 600^\circ\text{C}$ the calculated EDT values from Eq. (4) are 536°C EDT for the pinning term and 575°C EDT for the structure term. Because there are no values in the structure term table above 550°C EDT and interpolation is specified, the highest tabulated values, at 550°C EDT, were used for the structure term.

The existing fit is plotted as a dashed curve on Fig. 8, where it is clear that it does not fit the data as well as the new model based on actual T_{irr} . The existing fit is also plotted in Fig. 6 above for graphite group 2, with the same equivalence between measured T_{irr} and estimated EDT values. Additional comparisons were made in the other graphite groups for each temperature with sufficient data, and the conclusion is that the new model often provides a better fit in the range of dose and temperature covered by both models. The new model is also applicable at doses beyond the limit of the existing fit (i.e., $\geq 200 \times 10^{20} \text{ n/cm}^2$ EDND). The limit of applicability of the new model is given by the limit $DR < 1.8$ (the corresponding dose depends on T_{irr} as in Eq. (2)). The new model can also be used over a wider range in T_{irr} , and compares favorably with available data over the range $295^\circ\text{C} \leq T_{\text{irr}} \leq 600^\circ\text{C}$.

5. Conclusions

- An improved model based on an extensive irradiated Gilsocarbon database has been developed for estimating the increase in Young's modulus due to irradiation in inert environments. The new model provides a good fit to the available moderator graphite data over the range of the primary modelling variables: dose (up to at least $200 \times 10^{20} \text{ n/cm}^2$ EDND), irradiation temperature ($\sim 300\text{--}600^\circ\text{C}$), and graphite group.
- The new model has demonstrated predictive capability for data not used in fitting.
- The new model is often a better fit to the data than the existing model, for comparisons on inert environment data where both models are applicable. The new model is also applicable to higher dose and a broader temperature range than the existing model.
- The new model is more convenient because it is analytic in irradiation temperature and dose, eliminating the need for interpolation as is required with the existing Young's modulus model.

- The new model does not yet incorporate any effects of radiolytic oxidation, although model revisions to account for such effects are planned.
- Modulus data are available on Gilsocarbon at irradiation temperatures up to 1300 °C that could be considered for extending the model to temperatures of interest to the VHTR.

Acknowledgements

The authors would like to thank J. Reed and M. Bradford of British Energy for valuable review and commentary during the conduct of the work and preparation of this paper. The authors also

thank the UK Health and Safety Executive (Nuclear Safety Directorate) for financial support. The views expressed in this paper are those of the authors and do not necessarily represent those of the Health and Safety Executive or British Energy.

References

- [1] J.E. Brocklehurst, B.T. Kelly, Carbon 31 (1) (1993) 155.
- [2] J.V. Best, W.J. Stephen, Progr. Nucl. Energy 16 (2) (1985) 127.
- [3] UKAEA – Various reports written between 1947 and 1996, available from the UK public records office www.pro.gov.uk, filed under section AB.
- [4] E.D. Eason, G.N. Hall, B.J. Marsden, in: Proceeding of the Ageing Management of Graphite Reactor Cores Conference, Cardiff, 28–30 November 2005.
- [5] E.D. Eason, G.N. Hall, G.B. Heys, J.F. Knott, B.J. Marsden, S.D. Preston, T. Swan, J. Nucl. Mater. 381 (2008) 106.